HHS Public Access

Author manuscript

Int J Cardiol. Author manuscript; available in PMC 2018 April 09.

Published in final edited form as:

Int J Cardiol. 2017 April 01; 232: 233–242. doi:10.1016/j.ijcard.2017.01.013.

Essential role of ICAM-1 in aldosterone–induced atherosclerosis

Vincenzo Marzolla[1], **Andrea Armani**[1,*], **Caterina Mammi**[1,*], **Mary E. Moss**[2], **Vittoria Pagliarini**[3], **Laura Pontecorvo**[4], **Antonella Antelmi**[5], **Andrea Fabbri**[6], **Giuseppe Rosano**[7,8], **Iris Z. Jaffe**[2], and **Massimiliano Caprio**[1,9]

[1]Laboratory of Cardiovascular Endocrinology, IRCCS San Raffaele Pisana, Rome, Italy

[2]Molecular Cardiology Research Institute, Tufts Medical Center, Boston, Massachusetts, USA

[3]Department of Biomedicine and Prevention, University of Rome Tor Vergata, 00133 Rome, Italy Laboratory of Neuroembryology, Fondazione Santa Lucia, 00143 Rome, Italy

[4]Laboratory of Pathophysiology of Cachexia and Metabolism of Skeletal Muscle, IRCCS San Raffaele Pisana, Rome, Italy

[5]Interinstitutional Multidisciplinary Biobank (BioBIM), IRCCS San Raffaele Pisana, Via di Val Cannuta 247, 00166 Rome, Italy

[6]Department of Systems Medicine, Endocrinology Unit, S. Eugenio & CTO A. Alesini Hospitals-ASL RM2, University Tor Vergata, Rome, Italy

[7]Cardiovascular & Cell Science Institute, St George's Hospital NHS Trust, University of London, London, United Kingdom

[8]Department of Medical Sciences, IRCCS San Raffaele, Rome, Italy

[9]Department of Human Sciences and Promotion of the Quality of Life, San Raffaele Roma Open University, Rome, Italy

Abstract

Objective—Elevated aldosterone is associated with increased risk of atherosclerosis complications, whereas treatment with mineralocorticoid receptor (MR) antagonists decreases the rate of cardiovascular events. Here we test the hypothesis that aldosterone promotes early atherosclerosis by modulating intercellular adhesion molecule-1 (ICAM-1) expression and investigate the molecular mechanisms by which aldosterone regulates ICAM-1 expression.

Methods and Results—Apolipoprotein-E (ApoE)$^{-/-}$ mice fed an atherogenic diet and treated with aldosterone for 4 weeks showed increased vascular expression of ICAM-1, paralleled by

Corresponding author's contact: Professor M Caprio, Laboratory of Cardiovascular Endocrinology, IRCCS San Raffaele Pisana, Via di Val Cannuta 247, Rome 00166, Italy. massimiliano.caprio@sanraffaele.it.

*These authors contributed equally to this work.

Conflict of interests

The authors report no relationships that could be construed as a conflict of interest.

enhanced atherosclerotic plaque size in the aortic root. Moreover, aldosterone treatment resulted in increased plaque lipid and inflammatory cell content, consistent with an unstable plaque phenotype. ApoE/ICAM-1 double knockout ($ApoE^{-/-}$/$ICAM\text{-}1^{-/-}$) littermates were protected from the aldosterone-induced increase in plaque size, lipid content and macrophage infiltration. Since aldosterone is known to regulate ICAM-1 transcription via MR in human endothelial cells, we explored MR regulation of the ICAM-1 promoter. Luciferase reporter assays performed in HUVECs using deletion constructs of the human ICAM-1 gene promoter showed that a region containing a predicted MR-responsive element (MRE) is required for MR-dependent transcriptional regulation of ICAM-1.

Conclusions—Pro-atherogenic effects of aldosterone are mediated by increased ICAM-1 expression, through transcriptional regulation by endothelial MR. These data enhance our understanding of the molecular mechanism by which MR activation promotes atherosclerosis complications.

Keywords

Intercellular Adhesion Molecule-1; Aldosterone; Mineralocorticoid Receptor; Atherosclerosis

1. Introduction

Higher aldosterone (ALDO) levels are associated with increased risk of cardiovascular ischemic events and mortality [1–3]. For example, patients with primary hyperaldosteronism have a four or six fold increased incidence of stroke or myocardial infarction (MI), respectively, compared to patients with essential hypertension[4]. Even within the normal range, ALDO levels above the median predict a significantly increased risk of MI, stroke and death in patients with known coronary artery disease [2]. ALDO is also a significant independent predictor of progression of atherosclerosis in humans[5]. ALDO levels are increased in the growing populations with obesity, heart failure, and resistant hypertension [6–9] thus understanding the mechanism by which ALDO promotes cardiovascular ischemia has important clinical implications. ALDO acts by binding and activating the mineralocorticoid receptor (MR), a hormone activated transcription factor. Accordingly, randomized clinical trials reveal that treatment with MR antagonists (spironolactone or eplerenone) reduce cardiovascular events and improve survival in patients with heart failure [10,11].

Atherosclerosis is a chronic inflammatory disorder of the vasculature. In response to cardiovascular risk factors, the endothelium lining the vessel becomes damaged. This dysfunctional endothelium potentiates leukocyte adhesion and migration into the vessel wall [12,13]. Dysfunctional endothelial cells (EC) promote vascular inflammation by expressing surface adhesion molecules involved in the development of atherosclerotic plaques including intercellular adhesion molecule-1 (ICAM-1), vascular cell adhesion molecule-1 (VCAM-1) and endothelial cell selectin [14,15]. Intravascular leukocytes then take up lipids and form the core of the atherosclerotic plaque. Plaques with increased inflammatory cell infiltrate and lipid content are prone to rupture and thrombosis, and this vulnerable plaque phenotype is the cause of most MIs and strokes [16]. Thus, understanding mechanisms driving plaque progression and inflammation and the role of ALDO/MR, may explain the clinical

observations linking ALDO to cardiovascular ischemia. Animal studies support a role for ALDO and MR in the development of atherosclerosis. ALDO infusion into the apolipoprotein E knockout mouse ($ApoE^{-/-}$), a model prone to atherosclerosis, induced an increase in plaque size with increased plaque lipid and inflammatory cell content, similar to the vulnerable plaque in humans [17–19]. Conversely, MR antagonism reduced plaque development in $ApoE^{-/-}$mice [20–22].

The mechanism by which ALDO contributes to vascular inflammation and atherosclerosis is not clear. In a mouse model of diet-induced obesity, animals developed endothelial dysfunction by an ALDO-dependent mechanism, and this effect was prevented by MR antagonist treatment, implicating a role for the MR [23]. A role for MR in ECs is suggested by studies in mice with MR specifically deleted from ECs. These EC-MR knockout mice were protected from endothelial dysfunction induced by ALDO or Angiotensin II infusion or exposure to high fat diet-induced obesity [24–26]. We previously demonstrated that ALDO treatment of human coronary artery ECs increases ICAM-1 gene expression and in turn promotes leukocyte adhesion to cultured human coronary ECs. These effects were abolished by MR antagonists or by MR knock down in cultured ECs [27]. However, whether MR regulation of ICAM-1 expression contributes to vascular inflammation and atherosclerosis *in vivo* has never been investigated. ICAM-1 knockout mice showed reduced atherosclerosis development in the $ApoE^{-/-}$ model indicating an important role for ICAM-1 in the formation of atherosclerotic plaques [28]. In order to investigate if the atherogenic effects of ALDO are mediated by ICAM-1, we analyzed size and composition of atherosclerotic plaques in the aortic root of ALDO-infused double knockout mice ($ApoE^{-/-}$/$ICAM\text{-}1^{-/-}$). We observed that genetic deletion of ICAM-1 prevented the increase in plaque size, lipid content and plaque inflammation induced by ALDO. In addition, *in vitro* studies indicated that the presence of a MR binding-site in the promoter region of ICAM-1 gene was necessary for MR-induced ICAM-regulation.

2. Materials and Methods

2.1. Mouse Atherosclerosis model and serum analysis

Animal procedures were approved by the Italian National Institute of Health care and use committees. Mice deficient in both ApoE and ICAM1 gene were generated by mating $ApoE^{-/-}$mice with $ICAM\text{-}1^{-/-}$mice (C57BL/6 background).The resulting $ApoE^{-/-}$/$ICAM\text{-}1^{+/-}$ mice were intercrossed to produce $ApoE^{-/-}$/$ICAM\text{-}1^{-/-}$ mice and equivalent $ApoE^{-/-}$/ ICAM-1-intact littermates. In nine-week-old male mice were placed osmotic minipump (Alzet model 1004) subcutaneously containing vehicle (ethanol/saline) or aldosterone (6 μg/ mouse/day) for four-week. Over the 5 days prior to animal euthanasia, tail-cuff blood pressure and heart rate measurements were performed using the CODA mouse tail cuff System and software (Kent Scientific) by a 3-day training and measurement protocol that we have previously described and validated [29]. Prior to all surgical procedures, mice were anesthetized with 1.5% isofluorane. Animals undergoing survival surgeries received 0.05 mg/kg buprenorphine administered subcutaneously prior to incision, and additional doses at 8-hr intervals if deemed beneficial. At the time of minipump implantation, mice were placed on a proatherogenic HF diet (Harlan Teklad TD.88137). At the time of sacrifice, peripheral

blood samples were collected via retro-orbital bleeding. Fasting serum samples were assayed for glucose, cholesterol, sodium and potassium levels (Plaisant Srl Rome, Italy). ALDO serum was assayed (Siemens Health Care RIA) according to manufacturers' instructions.

2.2. Immunohistochemistry

At the time of euthanization, animals were fasted for 4 hours, and blood was collected from the inferior vena cava. Animals were then perfused with phosphate-buffered saline (PBS), and tissues were collected. The aortic valve were embedded in optimal cutting compound (OCT).

Cryosections of embedded aortic roots at the site where all 3 aortic valve leaflets could be visualized were taken at five-micron intervals. Sequential sections were stained with Oil-Red O (ORO), picrosirius red (PSR), anti-Mac3 antibody (BD Pharmingen) or anti-ICAM1 to quantify lipids, necrotic core, collagen content, activated inflammatory cells or ICAM1 expression in the aortic root at the level of the aortic valve. Total pixels staining positive for the component of interest were normalized to overall plaque area to generate fold increase respect to vehicle-treated mice. Images were collected and analyzed by a treatment blinded investigator using ImagePro Premier software (Media Cybernetics). ImagePro Premier software was also used to measure the necrotic core of each plaque (measured as percentage of the total plaque area).

2.3. Plasmids construction

3 Kb of human ICAM-1 promoter (NCBI Reference Sequence: NG_012083.1) was cloned into pGL3 BASIC vector (Promega) upstream of luciferase gene. Moreover four 5' deletion fragments of the 3Kb promoter (1500 bp, 1141 bp, - MRE and 872 bp) were generated employing appropriate restriction enzymes or PCR reaction and were cloned into pGL3 BASIC vector upstream of the firefly luciferase gene. The 1500 bp fragment was obtained by double digestion of 3 Kb promoter of ICAM-1 with SacI and NarI and cloned into into pGL3 BASIC vector previously digested with the same enzymes.

The 1141 bp, -MRE and 872 bp fragments were generated by PCR reaction performed with Pfu DNA Polymerase (Promega) employing as template the 3 Kb ICAM-1 promoter and using the following couples of primers:

F 1141 bp (GAAGAGCTCCCCGGGGAGGATTCCTGGGC) and

R 1141 bp (AATGGCGCCGGGCCTTTCTTTATGTTTT);

F - MRE (GAAGAGCTCAGGCGGCGCGGCTTGGTGCT) and

R - MRE (AATGGCGCCGGGCCTTTCTTTATGTTTT)

F 872 bp (GAAGAGCTCGGGTTTAATGCCGGTTTAC) and

R 872 bp (AATGGCGCCGGGCCTTTCTTTATGTTTT)

The PCR product was digested with SacI and NarI and cloned into pGL3 BASIC vector cut with the same enzymes. T4 DNA ligase (BioLabs) was used for cloning reactions.

2.4. Transfection of HUVEC and Luciferase Assay

Sixteen hours before transfection, 8×10^4 HUVECs were plated into 6-well cell culture plates with 2 ml of complete EGM-2 medium (Lonza). Two hours before transfection, cells were shifted into medium EGM-2 medium containing 2% stripped serum and deprived of hydrocortisone and gentamicine. For the transfection, 98 µl of EBM-2 (basal medium) and 3 µl of FUGENE 6 were added and gently mixed within a sterile tube and incubated for 5 minutes at room temperature. Then, 1 µg total of appropriate mixture of vectors (containing 980 ng of 3kb ICAM-1 plasmid or equimolar concentration of plasmids containing promoter's deletions and 20 ng of pRL-TK vector) were added in the tube and incubated for 1 hour at room temperature. The FUGENE 6/DNA complexes were then added to the cells in a drop-wise manner and cells returned to the incubator. The culture plates were incubated at 37°C and 5% CO_2 for two days. Twenty four hours after beginning of transfection, cells were treated as indicated in the figure 6 (aldo 10^{-8} M, aldo 10^{-8} M + SPIRO 10^{-5} M, SPIRO 10^{-5} M). Twenty four hours post treatment the cells were then washed twice with PBS and lysed with 250 µl of 1× Passive Lysis Buffer (Promega). The plates were rocked several time to ensure complete coverage of the cells with lysis buffer. Then the cells were scraped and the lysate was transferred into a microcentrifuge tube, vortexed and centrifuged at 12,000 × g for 2 minutes at 4°C. The supernatant was transferred into a new microcentrifuge tube.

For the Luciferase assay, 100 µl of Luciferase Assay Reagent II for each sample were dispensed into a white Optiplate 96 (PerkinElmer) and 20 µl of lysed product were added. Immediately the plate was read in a luminometer (Tecan Infinite 200) programmed to perform a 12-second measurement read for Firefly Luciferase activity. After this measurement, 100 µl of 1× Stop &Glo Reagent were added and the plate was briefly mixed. The plate was read again with a 12-second measurement for Renilla Luciferase activity (encoded bypRL-TK vector). The ratio of the Firefly: Renilla Luciferase activity represents the normalized reporter gene expression.

2.5. Adenovirus Infection and cell culture study

HUVECs were grown to 50% of confluence in complete EGM-2. Two hours before infection, cells were shifted into EBM-2 serum free. The cells were infected in triplicates with the control adenovirus which expresses the green fluorescent protein (Ad-GFP), or the adenovirus expressing the dominant negative-c-Jun form (Ad-dn-c-Jun), or the adenovirus expressing the dominant negative-IκBα (Ad-dn- IκBα). Eight hours post-infection, cells were shifted into EGM-2 medium containing 2% stripped serum and deprived of hydrocortisone and gentamicine. The cells were treated for 24 hours with ALDO 10^{-8} M, ALDO 10^{-8} M + SPIRO 10^{-5} M and SPIRO 10^{-5} M. At the end of pharmacological treatment, the cells were washed twice with 1 × PBS and immediately lysed in 1 ml of TRIzol Reagent (Invitrogen) for RNA extraction. In other experiments, after infection, the cells were transfected with 1141 bp ICAM-1 promoter vector and underwent aldosterone and SPIRO treatment as above indicated. At the end of treatments the cells were washed twice with 1 × PBS and lysed with 250 µl of 1× Passive Lysis Buffer (for luciferase assay).

In preliminary experiments, we examined GFP transgene expression in HUVECs infected with Ad-GFP at a MOI of 50, 100 or 200 or 500 by using fluorescence microscopy and found that GFP expression reaches 95% following adenoviral infection at 50 MOI.

2.6. RNA analysis

Cells and vascular tissue were washed twice with 1 × phosphate-buffered saline (PBS), harvested, and immediately lysed in 1 ml of TRIzol Reagent (Invitrogen). Total RNA was extracted following manufacturer's indications. The purity, integrity, and yield of RNA were analyzed by Agilent Technologies 2001 bioanalyzer using the RNA 6000 LabChip kit. One microgram of total RNA was treated with RQ1 RNase-Free DNase I (Promega) and reverse-transcribed using GoScript Reverse Transcription System (Promega). Quantitative PCR was performed in Mx3000P light cycler (Stratagene) using GoTaq qPCR Master Mix (Promega) as indicated by the manufacturer. All primers were optimized for real-time RT-PCR amplification checking the generation of a single peak in a melting curve assay and the efficiency in standard curve amplification (>98% for each primer pair).Target gene expression was normalized to 18S mRNA expression, the relative change in expression for each treatment was calculated by Mx3000P software version 2.0 (Stratagene) and is reported as arbitrary units. For all experiments each sample was analyzed in duplicate. Couples of primers used for real-time amplification are:

ICAM-1

F CAAGGCCTCAGTCAGTGTGA and

R CCTCTGGCTTCGTCAGAATC

TGF-β1

F TGCGCTTGCAGAGATTAAAA and

R CGTCAAAAGACAGCCACTCA

2.7. Flow cytometry assay

For flow cytometry at the end of each treatment the HUVECs were labeled with phycoerythrin-conjugated mouse antihuman ICAM1 monoclonal antibody or IgG1 isotype control. Mean fluorescence index was calculated by subtracting the isotype Ig control mean fluorescence from the ICAM1-stained mean fluorescence. Data are expressed as percentage of mean fluorescence index of vehicle-treated cells at each treatment time.

2.8. Western blot analysis

Specimens of aortic root (n=6 per genotype and treatment) were lysed in lysis buffer containing 1% Triton X-241 100, 50mM Hepes, 10% glycerol, 150mM NaCl, 1mM NaVO4 and 75 U of aprotinin. The lysates were subjected to polyacrylamide gel electrophoresis (SDS-PAGE), and transferred onto PVDF membranes. Membrane were probed with anti-PARP (Cell Signaling), or BCL-X (BD Pharmingen) or β-actin (Sigma-Aldrich) antibodies and horseradish peroxidase (HRP)-conjugated anti-rabbit IgG (Sigma-Aldrich, Milan, Italy). Immunoreactive bands were visualized using the ECL Western detection system (General

Electric Healthcare, Milan, Italy). Densitometric scanning analysis was performed by Mac OS X (Apple Computer International, Milan, Italy) using NIH 252 Image 1.62 software.

2.9. Statistical analysis

Data are reported as the mean +/− standard error of the mean. Data points greater or less than two standard deviations from the mean were considered statistical outliers and were excluded from all analyses. Statistical comparisons were made by t-test, one-way or two-way ANOVA followed by Bonferroni post hoc analysis using Prism 6.0 (GraphPad). $P<0.05$ was considered significant.

3. Results

3.1. ALDO infusion increases aortic ICAM-1 expression in an atherosclerosis model *in vivo*

In order to explore the role *in vivo* of ICAM-1 in ALDO-induced atherosclerosis, we generated ApoE$^{-/-}$/ICAM-1$^{-/-}$double knockout mice. Male ApoE$^{-/-}$/ICAM-1$^{-/-}$mice and ApoE$^{-/-}$/ICAM-1$^{+/+}$ littermates were fed an atherogenic high fat diet (HFD) and randomized to infusion with vehicle or ALDO for 4 weeks. After 4 weeks, ICAM-1 mRNA expression was quantified in whole aortic tissue. ALDO infusion significantly increased ICAM-1 mRNA expression in the aorta of ApoE$^{-/-}$/ICAM-1$^{+/+}$ mice compared to vehicle-treated ApoE$^{-/-}$/ICAM-1$^{+/+}$ mice (Fig.1A). As expected, ICAM-1 transcript levels were virtually undetectable in ApoE$^{-/-}$/ICAM-1$^{-/-}$ mice regardless of ALDO- or vehicle-treatment, validating ICAM-1 deletion in our mouse model. Consistent with the transcript profile, ICAM-1 protein expression was evident in atherosclerotic plaques in aortic root sections of vehicle- and ALDO-treated ApoE$^{-/-}$/ICAM-1$^{+/+}$ mice, as shown by immunostaining for ICAM-1 (Figure 1B). As expected ApoE$^{-/-}$/ICAM-1$^{-/-}$ mice, did not show any ICAM-1 staining.

3.2. ICAM-1 is required for ALDO-enhanced atherosclerotic plaque formation

As previously demonstrated [17], low dose of ALDO infusion (6 μg/mouse per day) significantly increased early atherosclerotic plaque formation in the aortic root of ApoE$^{-/-}$ mice fed an atherogenic diet for 4 weeks (Figure 2).This dose of ALDO was chosen because it produces a 3- to 5-fold elevation in serum ALDO levels, similar to that seen in patients with cardiovascular risk factors [6–8]. This level of ALDO did not cause any significant change in blood pressure, body weight, or serum total cholesterol (Table 1). Importantly, littermates lacking ICAM-1 were protected from the ALDO-induced increase in plaque burden (Figure 2). These data support the concept that at levels that do not increase blood pressure, ALDO increases aortic ICAM-1 expression in high fat fed ApoE$^{-/-}$ mice and that ICAM-1 is necessary for ALDO-induced atherosclerosis (Figure 2).

3.3. ICAM-1 is necessary for ALDO induction of a vulnerable plaque phenotype

Plaque composition was next investigated in histological sections of aortic root from ALDO- or vehicle-treated ApoE$^{-/-}$/ICAM-1$^{+/+}$ and ApoE$^{-/-}$/ICAM-1$^{-/-}$littermates. The fraction of the plaque that is composed of lipids or necrotic core was quantified in Oil Red O stained sections (Figure 2) and the inflammatory cell and collagen component was quantified in serial sections of aortic root stained with anti-Mac3 antibody or Sirius Red, respectively

(Figure 3). As previously demonstrated, in mice with intact ICAM-1, ALDO treatment resulted in plaques with a significant increase in lipid content (2.1 fold, Figure 2C). ALDO did not affect the percent necrotic core (Figure 2D) or markers of apoptosis (Supplemental Figure 1). ALDO also increased activated inflammatory cell-positive area (2.1 fold, Figure 3A) compared with vehicle-treated ApoE$^{-/-}$/ICAM-1$^{+/+}$ mice. Plaque fibrosis as measured by collagen content did not differ among treatment groups (Figure 3B) nor did ALDO alter TGF-β1 transcript levels by real time RT-PCR in samples of aortic root (Supplemental Figure 2). Overall ALDO produced a plaque phenotype with increased lipids and inflammation with no change in necrosis and fibrosis. Importantly, the ALDO-induced increase in plaque lipid content and inflammation was prevented in ApoE$^{-/-}$/ICAM-1$^{-/-}$ mice (Figure2B and 3A, respectively), indicating that ICAM-1 is necessary to mediate the effects of ALDO on plaque phenotype.

3.4. ALDO regulates ICAM-1 expression in human endothelial cells by MR-dependent transcriptional control

To explore the mechanism by which ALDO regulates endothelial ICAM-1expression, we first examined ALDO regulation of ICAM-1 mRNA expression in human umbilical vein ECs (HUVEC). Transcript levels of ICAM-1 were analyzed by qRT-PCR in HUVECs treated with ALDO (10^{-8}M) in presence or absence of the MR antagonist spironolactone (SPIRO, 10^{-5}M), in serum lacking steroid hormones. ALDO treatment of HUVECs for 24 hours resulted in a significant increase in ICAM-1 mRNA expression (1.5 fold) and this was significantly inhibited by SPIRO (Figure 4A), supporting a MR-dependent mechanism. In addition to transcriptional regulation, ALDO is also capable of exerting rapid non-genomic effects on vascular cells [30,31]. In order to explore potential non-genomic effects of ALDO on ICAM-1 surface protein expression, HUVECs were treated with ALDO (10^{-8}M) for 30 minutes, 1 hour, 3 hours, 24 hours in the presence or absence of SPIRO (10^{-5}M) and surface ICAM-1 protein levels were quantified by flow cytometry. ALDO did not significantly increase ICAM-1 protein surface expression between 30 minutes and 3 hours making non-genomic effects on ICAM-1 membrane trafficking an unlikely mechanism. In accordance with the qPCR studies, ALDO treatment significantly increased surface ICAM-1 protein after 24 hours, (Figure 4B). This increase was prevented by co-treatment with SPIRO. These data support a model in which ALDO regulates ICAM-1 expression in HUVECs through a genomic mechanisms that requires endothelial MR.

3.5. Promoter analysis of human ICAM-1 gene in HUVECs

To further investigate the transcriptional regulation of ICAM-1 by ALDO, luciferase reporter assays were performed in HUVECs after transient transfection with a reporter vector containing the 3kb proximal promoter region of the human ICAM-1 gene. ALDO treatment (10^{-8}M) significantly increased the activity of the 3kb ICAM-1 promoterfragment (Figure 5A) to a similar extent as the ALDO-induced increased ICAM-1 mRNA expression (Figure 4A). This effect on ICAM-1 promoter activity was inhibited by the co-treatment with SPIRO (10^{-5}M) (Figure 5A), supporting a MR-dependent mechanism for ALDO regulation of ICAM-1 transcription.

Serial 5'-deletions of the ICAM-1 promoter fragment were prepared to identify sequences critical for ALDO-regulation of ICAM-1 promoter activity. Figure 5B shows the deleted ICAM-1 promoter fragments used in the transfection experiments. ALDO administration significantly increased the activity of the 1500 bp and the 1141 bp ICAM-1 promoter fragments (1.8 and 2.2 fold, respectively), without affecting the activity of the 872 bp construct (Figure 5C).The ALDO-mediated increase was inhibited by co-treatment with SPIRO. Altogether these data identify putative sequences localized in the region of ICAM-1 promoter comprised between 1141 and 872 bp that are necessary for MR activation of the ICAM-1 promoter (Figure 5C).

3.6. A mineralocorticoid responsive element (MRE) in the ICAM-1 promoter is necessary for MR-dependent transcriptional regulation

To identify putative binding sites for transcription factors that may be involved in modulation of ICAM-1 gene expression induced by ALDO, we performed bioinformatic analysis (database on jasper.genereg.net) of the promoter region between nucleotides −1141 and −872. The analysis showed the presence of putative binding sites for MR, NF-κB and AP-1 (Figure 6A). In order to determine if the MRE mediates ALDO responsiveness of the 1141 bp ICAM-1 promoter fragment, we first generated an 1141bp promoter fragment lacking the putative MRE. Transcriptional analysis showed that the absence of the MRE completely blocked the ALDO-induced promoter activity (Figure 6B). The promoter activity in the absence of MRE was comparable to that of the 872bp construct. We also examined the involvement of NF-κB and c-Jun (a component of the AP-1 transcription factor) by analyzing ALDO responsiveness of the 1141 bp promoter after adenovirus infection with dominant negative constructs for c-Jun (Ad-dn-c-Jun) or for NF-κB (Ad-dn-IκBα). A viral construct expressing Ad-GFP was used as control. Interestingly, cells infected with Ad-dn-c-Jun and Ad-dn- IκBα (50 MOI) displayed blunted 1141bp ICAM-1 promoter activity, induced by ALDO, compared to control infection with Ad-GPF (Figure 6C), suggesting that c-Jun and NF-κB may contribute in part to the regulation of ICAM-1 promoter activity by MR in human ECs.

4. Discussion

This study reveals a fundamental role for ICAM-1 in ALDO induction of early atherosclerosis and supports a novel mechanism by which blood pressure–independent effects of ALDO promote early development of vascular inflammation and atherosclerotic plaque formation. Specifically, we demonstrated for the first time *in vivo* that ALDO enhances vascular ICAM-1 expression in the aorta of $ApoE^{-/-}$ mice and that ICAM-1 is necessary for ALDO to increase aortic root plaque size and lipid and inflammatory cell content independent of blood pressure. In addition, we show that ALDO regulates ICAM-1 expression in human ECs by activating EC MR and enhancing ICAM-1 transcription via a MRE in the human ICAM-1 proximal promoter.

A robust body of evidence demonstrates that plasma levels of ALDO represent an independent predictor of cardiovascular ischemia [5]. In fact, it has been shown that higher ALDO levels, even within the normal range, predict a significant increase in myocardial

infarction and cardiovascular death, in patients with atherosclerosis [2]. A recent study on the general population reported that ALDO levels were associated with hypertension, visceral obesity, metabolic syndrome, high triglycerides, concentric left ventricular hypertrophy, and increased mortality. Importantly, this association persisted even after adjustment for body mass index and after excluding subjects with ALDO levels above the normal range [32]. Thus, ALDO levels are elevated in growing populations at high risk for cardiovascular ischemic events and, even in the general population, predicts poor cardiovascular outcomes by mechanisms that are not totally clear.

In the present study we used a dose of ALDO that produced a modest, but clinically relevant, increase in serum ALDO, to mimic ALDO plasma level of patients with cardiovascular diseases [17], and then characterized atherosclerotic plaque burden in ApoE$^{-/-}$/ICAM-1$^{+/+}$ and ApoE$^{-/-}$/ICAM-1$^{-/-}$ mice treated for 4 weeks and fed a HFD. Importantly, ALDO treatment at this dose did not increase systolic blood pressure, nor did it alter metabolic parameters known to affect cardiovascular risk (body weight, total cholesterol, glucose, Table1), excluding confounding hemodynamic and metabolic factors that could have altered the atherosclerotic process. This suggests a direct effect of ALDO on the vasculature that we suggest may be mediated by activation of MR in the endothelium to up-regulate ICAM-1. This is consistent with our data showing that this dose of ALDO significantly increased ICAM-1 transcript levels in whole aorta independent of changes in blood pressure.

Moreover, we showed for the first time that ApoE$^{-/-}$/ICAM-1$^{-/-}$ mice are resistant to develop early atherosclerosis induced by ALDO treatment for 4 weeks. Perhaps more importantly, the ALDO-induced increase in plaque lipid and inflammatory cell content was also prevented in mice lacking ICAM-1. This has important clinical implications since a plaque phenotype with increased lipids and inflammatory cells is known to contribute to susceptibility to rupture, the cause of most MIs and strokes [16]. This mechanism may therefore explain the increased risk of MI and stroke in patients with elevated ALDO levels [2,4].

Since ICAM-1 is a known mediator of atherogenesis, it may seem surprising that we found no difference in the plaque burden in the vehicle treated animals lacking ICAM-1. This apparent discrepancy is likely explained by the early time frame with only 4 weeks of treatment with high fat diet. This is consistent with a previous paper by Bourdillon *et al.* which investigated the effects of the lack of the ICAM-1 gene on atherosclerosis development in ApoE−/− mice [28]. In this work, the authors analyzed the atherosclerotic plaque size in the aortic arch region of ApoE$^{-/-}$/ICAM-1$^{-/-}$ (DKO) and ApoE$^{-/-}$/ICAM-1$^{+/+}$ (KO) mice fed chow or HFD for 3, 6, 15, 20 weeks. DKO and KO mice fed HFD for 6 weeks showed comparable atherosclerosis, indicating that the lack of ICAM-1 gene does not affect plaque burden at this early time. On the other hand, Bourdillon *et al.* observe that, after a longer treatment with HFD, DKO mice displayed reduced atherosclerosis compared with KO mice, indicating that the atherosclerotic burden observed after 15 weeks of HFD is affected by the presence of ICAM-1. Overall, the data supports that ALDO promotes early plaque development and inflammation by upregulation of ICAM-1 and that even in the absence of exogenous ALDO, ICAM-1 further contributes to late plaque burden.

In the vasculature, ECs express several adhesion molecules, including ICAM-1, involved in early steps of atherosclerosis. Whether the EC-MR-ICAM1 pathway plays an important role in inflammation in vivo has been controversial [33]. A mouse lacking MR in ECs and leukocytes developed less inflammation and macrophage recruitment into cardiac tissue in response to mineralocorticoid-induced hypertension [34]. Another study showed that ALDO treatment increases ICAM-1 in rat heart, leading to inflammatory arterial lesions [35]. While these studies suggested a role for EC-MR regulation of ICAM in cardiac inflammation, in another study examining cardiac inflammation in response to pressure overload induced by trans-aortic constriction, ICAM-1 levels in the heart increase and contribute to cardiac inflammation but this was not affected by specific deletion of MR only from ECs [36]. The current study is the first to evaluate the role of ICAM-1 regulation by MR in atherosclerosis and vascular inflammation *in vivo*.

Since EC adhesion molecules contribute to vascular inflammation and atherosclerosis in animal models and humans, studies have examined whether these proteins could be biomarkers to predict ischemic events. Some studies have shown an association between serum levels of adhesion molecules and plaque stability. For example, Hoke *et al*. identified soluble ICAM-1 and VCAM-1 as predictors of cardiovascular events in patients with stable carotid atherosclerosis [37]. However, the prognostic significance of soluble ICAM-1 (sICAM-1) in the cardiovascular diseases is still controversial with some studies showing patients with higher circulating levels of sICAM-1 having increased number of cardiovascular events [38,39] and others finding no relationship between sICAM-1 and the risk of cardiovascular events [40]. Thus further studies are needed to determine if circulating adhesion molecules will be a clinically valuable biomarker of risk or perhaps serum aldosterone levels may be more predictive.

In addition to transcriptional regulation, MR is known to modulate the expression of target genes through rapid non-genomic activation of protein kinases and secondary messenger signaling pathways [41]. To clarify the mechanisms by which endothelial MR regulates ICAM-1, we explored the time course of the increase in EC ICAM-1 surface protein expression in response to ALDO. We confirmed that 24-hours of ALDO treatment increased transcript levels of ICAM-1 and that SPIRO prevented such effect, consistent with prior studies [27,34]. Increased surface protein expression of ICAM-1 was detected after 24 hours of ALDO treatment but not after 30 minutes to 3 hours, excluding the involvement of rapid non-genomic effects of ALDO in the control of ICAM-1 surface protein expression.

To date, despite the large body of evidence that links MR activation with pro-inflammatory phenotype [17,42], only few studies have investigated the molecular mechanism by which MR directly interacts with pro-inflammatory gene promoters. In vascular smooth muscle and mesangial cells, it has been observed that ALDO is able to activate NF-κB and AP-1 (heterodymer of c-Jun/c-Fos) to induce inflammatory responses [43,44], but the molecular mechanism through which ALDO induces ICAM-1 transcription in human ECs has not previously been elucidated. In cultured mesangial cells, it was shown that ALDO stimulates ICAM-1 gene expression through Serum-Glucocorticoid Regulated Kinase 1/NF-κB signaling [45]. Conversely, in neutrophil cell cultures, ALDO decreases ICAM-1 expression by inhibiting NF-κB pathway [46]. These studies indicate that inflammatory pathways

downstream MR may vary depending on the cell type and environment. Therefore we sought to investigate mechanisms controlling ICAM-1 transcription in response to ALDO in human ECs. Our analysis of the human ICAM-1 promoter identified a novel MRE and two closely adjacent binding sites for NF-κB and AP-1. We demonstrated that specific deletion of MRE in human ICAM-1 promoter leads to complete inhibition of promoter activity induced by ALDO, indicating this MRE as essential for MR-induced ICAM-1 gene expression. Inability of several MR antibodies that we tested to immunoprecipitate MR in HUVECs or HEK293T (human embryonic kidney, expressing high level of MR) cell lines, did not allow us to perform chromatin immunoprecipitation assay to demonstrate direct binding of MR to the endogenous ICAM-1 promoter region, and this represents a limitation of our study.

Using adenovirus expressing dominant negative for c-Jun and NF-kB, we also observed that inhibition of each of these two transcription factors does not completely abolish MR-induced ICAM-1 transcription but rather partially attenuated the effect of ALDO. These data suggest a mechanism in which NF-kB and AP1 play a permissive role in MR-mediated regulation of ICAM-1 transcription that requires the MRE. This suggests that in ECs, ALDO regulates ICAM-1 transcription by a mechanism that differs from that in mesangial cells [45].

Several additional limitations of our study should be pointed out. First, all studies were performed in male mice. As the incidence and outcomes from atherosclerotic vascular disease differ in males and females, and studies show that estrogen receptor may modulate MR regulation of ICAM-1 in endothelial cells [47], future studies are needed to explore whether this mechanism contributes to plaque formation in females. Another limitation stems from the lack of investigation of macrophages ICAM-1 expression in response to ALDO, which could also contribute to explain the pro-atherogenic effects of ALDO [48]. In fact, MR is expressed in macrophages and affects their M1/M2 polarization and cardiac infiltration [49–51]. Notably, monocytes undergo macrophage activation in atherosclerotic lesions and contribute differently to the evolution of the plaque [52]. We did not quantify the smooth muscle cell component of the plaques since recent studies suggest that traditional smooth muscle cell markers are down-regulated in plaque SMCs thereby preventing accurate quantification of SMC without lineage tracing [53]. Finally, we did not measure HDL and LDL levels in serum samples, since the volume of serum obtained from mice was not enough to include these measurements.

Despite these limitations, our study broadens the possibility of therapeutic use of MR antagonists in different clinical settings, well beyond primary aldosteronism and resistant hypertension [54]. Since we show the critical relevance of endothelial MR activation by ALDO in the induction of ICAM-1 expression, vascular inflammation, and formation of vulnerable atherosclerotic plaques, this may be relevant in new populations of patients. Pharmacological blockade of the MR could be considered to prevent adverse cardiovascular outcomes in patients with obesity, metabolic syndrome, or known atherosclerotic vascular disease, where the risk of myocardial infarction or stroke is increased and independently associated with plasma ALDO levels. In this context, it is important to remark that the current normal values for ALDO do not take into account sensitivity of the endothelium to ALDO at levels that do not increase blood pressure and that the adverse cardiovascular effects of ALDO occur when plasma levels are inappropriate for salt status [55]. Finally, this

study identifies transcriptional up-regulation of ICAM-1 by endothelial MR as a novel mechanism that may contribute to the association of ALDO with risk of cardiovascular ischemia and highlights the clinical relevance of pharmacological MR antagonism to prevent atherosclerosis in patients with high cardiovascular risk.

Supplementary Material

Refer to Web version on PubMed Central for supplementary material.

Acknowledgments

The authors wish to thank Mark Aronovitz and Carol Galayda for technical teaching and assistance to A.A. for atherosclerosis studies, Andrea Marcello Isidori and Mary Anna Venneri for tail cuff analysis of blood pressure. We also thank Claudio Sette for fruitful discussion and scientific support. We would like to acknowledge networking support by the COST Action ADMIRE BM1301. This work was supported by a grant from Ministero della Salute (BANDO 2011–2012 Progetti Collaborazione Ricercatori Italiani all'Estero; project grant PE-2011-02347070 to M.C.) and by a grant from the National Institutes of Health ((HL095590) to IZJ).

Nonstandard Abbreviations and Acronyms

ALDO	aldosterone
MI	myocardial infarction
MR	mineralocorticoid receptor
EC	endothelial cell
ICAM-1	intercellular adhesion molecule 1
VCAM-1	vascular cell adhesion molecule 1
ApoE	apolipoprotein E
HFD	high fat diet
SPIRO	spironolactone
MRE	mineralocorticoid responsive element
NF-κB	nuclear factor kappa-light-chain-enhancer of activated B cells
AP-1	activator protein 1
HUVEC	human umbilical vein endothelial cell
TGFβ	Transforming growth factor β

References

1. Beygui F, Collet JP, Benoliel JJ, et al. High plasma aldosterone levels on admission are associated with death in patients presenting with acute ST-elevation myocardial infarction. Circulation. 2006; 114:2604–2610. [PubMed: 17116769]

2. Ivanes F, Susen S, Mouquet F, et al. Aldosterone, mortality, and acute ischaemic events in coronary artery disease patients outside the setting of acute myocardial infarction or heart failure. Eur. Heart J. 2012; 33:191–202. [PubMed: 21719456]

3. Tomaschitz A, Pilz S, Ritz E, et al. Association of plasma aldosterone with cardiovascular mortality in patients with low estimated GFR: the Ludwigshafen Risk and Cardiovascular Health (LURIC) Study. Am. J. Kidney Dis. 2011; 57:403–414. [PubMed: 21186074]

4. Milliez P, Girerd X, Plouin PF, et al. Evidence for an increased rate of cardiovascular events in patients with primary aldosteronism. J. Am. Coll. Cardiol. 2005; 45:1243–1248. [PubMed: 15837256]

5. de Rita O, Hackam DG, Spence JD. Effects of aldosterone on human atherosclerosis: plasma aldosterone and progression of carotid plaque. Can. J. Cardiol. 2012; 28:706–711. [PubMed: 22717248]

6. Bentley-Lewis R, Adler GK, Perlstein T, et al. Body mass index predicts aldosterone production in normotensive adults on a high-salt diet. J. Clin. Endocrinol. Metab. 2007; 92:4472–4475. [PubMed: 17726083]

7. Laffin LJ, Majewski C, Liao C, et al. Relationship Between Obesity, Hypertension, and Aldosterone Production in Postmenopausal African American Women: A Pilot Study. J. Clin. Hypertens. (Greenwich.). 2016

8. Calhoun DA. Aldosteronism and hypertension. Clin. J. Am. Soc. Nephrol. 2006; 1:1039–1045. [PubMed: 17699324]

9. Bansal S, Lindenfeld J, Schrier RW. Sodium retention in heart failure and cirrhosis: potential role of natriuretic doses of mineralocorticoid antagonist? Circ. Heart Fail. 2009; 2:370–376. [PubMed: 19808361]

10. Pitt B, Zannad F, Remme WJ, et al. The effect of spironolactone on morbidity and mortality in patients with severe heart failure. Randomized Aldactone Evaluation Study Investigators. N. Engl. J. Med. 1999; 341:709–717. [PubMed: 10471456]

11. Pitt B, Remme W, Zannad F, et al. Eplerenone, a selective aldosterone blocker, in patients with left ventricular dysfunction after myocardial infarction. N. Engl. J. Med. 2003; 348:1309–1321. [PubMed: 12668699]

12. Davignon J, Ganz P. Role of endothelial dysfunction in atherosclerosis. Circulation. 2004; 109:III27–III32. [PubMed: 15198963]

13. Hansson GK, Hermansson A. The immune system in atherosclerosis. Nat. Immunol. 2011; 12:204–212. [PubMed: 21321594]

14. Poston RN, Haskard DO, Coucher JR, et al. Expression of intercellular adhesion molecule-1 in atherosclerotic plaques. Am. J. Pathol. 1992; 140:665–673. [PubMed: 1372160]

15. Iiyama K, Hajra L, Iiyama M, et al. Patterns of vascular cell adhesion molecule-1 and intercellular adhesion molecule-1 expression in rabbit and mouse atherosclerotic lesions and at sites predisposed to lesion formation. Circ. Res. 1999; 85:199–207. [PubMed: 10417402]

16. Moss ME, Jaffe IZ. Mineralocorticoid Receptors in the Pathophysiology of Vascular Inflammation and Atherosclerosis. Front Endocrinol. (Lausanne). 2015; 6:153. [PubMed: 26441842]

17. McGraw AP, Bagley J, Chen WS, et al. Aldosterone increases early atherosclerosis and promotes plaque inflammation through a placental growth factor-dependent mechanism. J. Am. Heart Assoc. 2013; 2:e000018. [PubMed: 23525413]

18. Keidar S, Kaplan M, Pavlotzky E, et al. Aldosterone administration to mice stimulates macrophage NADPH oxidase and increases atherosclerosis development: a possible role for angiotensin-converting enzyme and the receptors for angiotensin II and aldosterone. Circulation. 2004; 109:2213–2220. [PubMed: 15123520]

19. Bodary PF, Sambaziotis C, Wickenheiser KJ, et al. Aldosterone promotes thrombosis formation after arterial injury in mice. Arterioscler. Thromb. Vasc. Biol. 2006; 26:233. [PubMed: 16373624]

20. Keidar S, Hayek T, Kaplan M, et al. Effect of eplerenone, a selective aldosterone blocker, on blood pressure, serum and macrophage oxidative stress, and atherosclerosis in apolipoprotein E-deficient mice. J. Cardiovasc. Pharmacol. 2003; 41:955–963. [PubMed: 12775976]

21. Raz-Pasteur A, Gamliel-Lazarovich A, Coleman R, et al. Eplerenone reduced lesion size in early but not advanced atherosclerosis in apolipoprotein E-deficient mice. J. Cardiovasc. Pharmacol. 2012; 60:508–512. [PubMed: 23232789]
22. Raz-Pasteur A, Gamliel-Lazarovich A, Gantman A, et al. Mineralocorticoid receptor blockade inhibits accelerated atherosclerosis induced by a low sodium diet in apolipoprotein E-deficient mice. J. Renin. Angiotensin. Aldosterone. Syst. 2014; 15:228–235. [PubMed: 23223089]
23. Huby AC, Antonova G, Groenendyk J, et al. Adipocyte-Derived Hormone Leptin Is a Direct Regulator of Aldosterone Secretion, Which Promotes Endothelial Dysfunction and Cardiac Fibrosis. Circulation. 2015; 132:2134–2145. [PubMed: 26362633]
24. Schafer N, Lohmann C, Winnik S, et al. Endothelial mineralocorticoid receptor activation mediates endothelial dysfunction in diet-induced obesity. Eur. Heart J. 2013; 34:3515–3524. [PubMed: 23594590]
25. Jia G, Habibi J, Aroor AR, et al. Endothelial Mineralocorticoid Receptor Mediates Diet-Induced Aortic Stiffness in Females. Circ. Res. 2016; 118:935–943. [PubMed: 26879229]
26. Mueller KB, Bender SB, Hong K, et al. Endothelial Mineralocorticoid Receptors Differentially Contribute to Coronary and Mesenteric Vascular Function Without Modulating Blood Pressure. Hypertension. 2015; 66:988–997. [PubMed: 26351033]
27. Caprio M, Newfell BG, la SA, et al. Functional mineralocorticoid receptors in human vascular endothelial cells regulate intercellular adhesion molecule-1 expression and promote leukocyte adhesion. Circ. Res. 2008; 102:1359–1367. [PubMed: 18467630]
28. Bourdillon MC, Poston RN, Covacho C, et al. ICAM-1 deficiency reduces atherosclerotic lesions in double-knockout mice (ApoE(−/−)/ICAM-1(−/−)) fed a fat or a chow diet. Arterioscler. Thromb. Vasc. Biol. 2000; 20:2630–2635. [PubMed: 11116064]
29. Jaffe IZ, Newfell BG, Aronovitz M, et al. Placental growth factor mediates aldosterone-dependent vascular injury in mice. J. Clin. Invest. 2010; 120:3891–3900. [PubMed: 20921624]
30. Schmidt BM, Sammer U, Fleischmann I, et al. Rapid nongenomic effects of aldosterone on the renal vasculature in humans. Hypertension. 2006; 47:650–655. [PubMed: 16520409]
31. Losel R, Schultz A, Boldyreff B, et al. Rapid effects of aldosterone on vascular cells: clinical implications. Steroids. 2004; 69:575–578. [PubMed: 15288772]
32. Buglioni A, Cannone V, Cataliotti A, et al. Circulating aldosterone and natriuretic peptides in the general community: relationship to cardiorenal and metabolic disease. Hypertension. 2015; 65:45–53. [PubMed: 25368032]
33. Caprio M, Mammi C, Jaffe IZ, et al. The mineralocorticoid receptor in endothelial physiology and disease: novel concepts in the understanding of erectile dysfunction. Curr. Pharm. Des. 2008; 14:3749–3757. [PubMed: 19128227]
34. Rickard AJ, Morgan J, Chrissobolis S, et al. Endothelial cell mineralocorticoid receptors regulate deoxycorticosterone/salt-mediated cardiac remodeling and vascular reactivity but not blood pressure. Hypertension. 2014; 63:1033–1040. [PubMed: 24566081]
35. Rocha R, Rudolph AE, Frierdich GE, et al. Aldosterone induces a vascular inflammatory phenotype in the rat heart. Am. J. Physiol Heart Circ. Physiol. 2002; 283:H1802–H1810. [PubMed: 12384457]
36. Salvador M, Nevers T, Velázquez F, et al. Intercellular Adhesion Molecule 1 Regulates Left Ventricular Leukocyte Infiltration, Cardiac Remodeling, and Function in Pressure Overload-Induced Heart Failure. J. Am. Heart Assoc. 2016; 5:e003126. [PubMed: 27068635]
37. Hoke M, Winter MP, Wagner O, et al. The impact of selectins on mortality in stable carotid atherosclerosis. Thromb. Haemost. 2015; 114:632–638. [PubMed: 25994120]
38. Hwang SJ, Ballantyne CM, Sharrett AR, et al. Circulating adhesion molecules VCAM-1, ICAM-1, and E-selectin in carotid atherosclerosis and incident coronary heart disease cases: the Atherosclerosis Risk In Communities (ARIC) study. Circulation. 1997; 96:4219–4225. [PubMed: 9416885]
39. Bonaterra GA, Zugel S, Kinscherf R. Novel systemic cardiovascular disease biomarkers. Curr. Mol. Med. 2010; 10:180–205. [PubMed: 20196728]
40. Postadzhiyan AS, Tzontcheva AV, Kehayov I, et al. Circulating soluble adhesion molecules ICAM-1 and VCAM-1 and their association with clinical outcome, troponin T and C-reactive

protein in patients with acute coronary syndromes. Clin. Biochem. 2008; 41:126–133. [PubMed: 18061588]

41. Dooley R, Harvey BJ, Thomas W. Non-genomic actions of aldosterone: from receptors and signals to membrane targets. Mol. Cell Endocrinol. 2012; 350:223–234. [PubMed: 21801805]
42. Krug AW, Allenhofer L, Monticone R, et al. Elevated mineralocorticoid receptor activity in aged rat vascular smooth muscle cells promotes a proinflammatory phenotype via extracellular signal-regulated kinase 1/2 mitogen-activated protein kinase and epidermal growth factor receptor-dependent pathways. Hypertension. 2010; 55:1476–1483. [PubMed: 20421514]
43. Zhu CJ, Wang QQ, Zhou JL, et al. The mineralocorticoid receptor-p38MAPK-NFkappaB or ERK-Sp1 signal pathways mediate aldosterone-stimulated inflammatory and profibrotic responses in rat vascular smooth muscle cells. Acta Pharmacol. Sin. 2012; 33:873–878. [PubMed: 22659623]
44. Han JS, Choi BS, Yang CW, et al. Aldosterone-induced TGF-beta1 expression is regulated by mitogen-activated protein kinases and activator protein-1 in mesangial cells. J. Korean Med. Sci. 2009; 24(Suppl):S195–S203. [PubMed: 19194552]
45. Terada Y, Ueda S, Hamada K, et al. Aldosterone stimulates nuclear factor-kappa B activity and transcription of intercellular adhesion molecule-1 and connective tissue growth factor in rat mesangial cells via serum- and glucocorticoid-inducible protein kinase-1. Clin. Exp. Nephrol. 2012; 16:81–88. [PubMed: 22042038]
46. Bergmann A, Eulenberg C, Wellner M, et al. Aldosterone abrogates nuclear factor kappaB-mediated tumor necrosis factor alpha production in human neutrophils via the mineralocorticoid receptor. Hypertension. 2010; 55:370–379. [PubMed: 20065153]
47. Barrett MK, Lu Q, Mohammad NN, et al. Estrogen receptor inhibits mineralocorticoid receptor transcriptional regulatory function. Endocrinology. 2014; 155:4461–4472. [PubMed: 25051445]
48. Yang M, Liu J, Piao C, et al. ICAM-1 suppresses tumor metastasis by inhibiting macrophage M2 polarization through blockade of efferocytosis. Cell Death. Dis. 2015; 6:e1780. [PubMed: 26068788]
49. Usher MG, Duan SZ, Ivaschenko CY, et al. Myeloid mineralocorticoid receptor controls macrophage polarization and cardiovascular hypertrophy and remodeling in mice. J. Clin. Invest. 2010; 120:3350–3364. [PubMed: 20697155]
50. Bienvenu LA, Morgan J, Rickard AJ, et al. Macrophage mineralocorticoid receptor signaling plays a key role in aldosterone-independent cardiac fibrosis. Endocrinology. 2012; 153:3416–3425. [PubMed: 22653557]
51. Bene NC, Alcaide P, Wortis HH, et al. Mineralocorticoid receptors in immune cells: emerging role in cardiovascular disease. Steroids. 2014; 91:38–45. [PubMed: 24769248]
52. Mantovani A, Garlanda C, Locati M. Macrophage diversity and polarization in atherosclerosis: a question of balance. Arterioscler. Thromb. Vasc. Biol. 2009; 29:1419–1423. [PubMed: 19696407]
53. Shankman LS, Gomez D, Cherepanova OA, et al. KLF4-dependent phenotypic modulation of smooth muscle cells has a key role in atherosclerotic plaque pathogenesis. Nat. Med. 2015; 21:628–637. [PubMed: 25985364]
54. Clark D III, Ahmed MI, Calhoun DA. Resistant hypertension and aldosterone: an update. Can. J. Cardiol. 2012; 28:318–325. [PubMed: 22521297]
55. Funder JW. Sensitivity to aldosterone: plasma levels are not the full story. Hypertension. 2014; 63:1168–1170. [PubMed: 24711520]

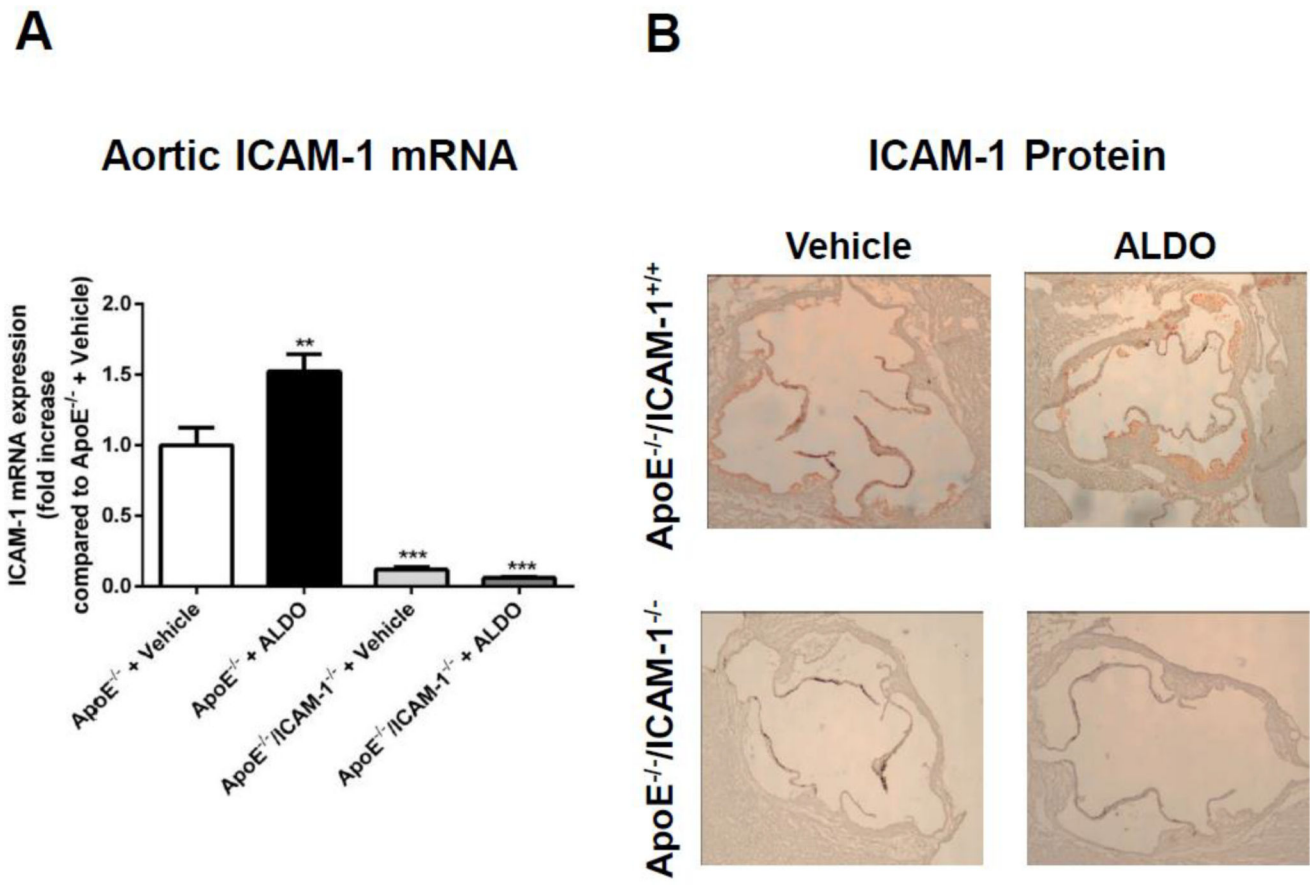

Fig. 1. ALDO infusion in ApoE$^{-/-}$ mice induces aortic ICAM-1 expression

Aldosterone (ALDO) or vehicle was infused into ApoE$^{-/-}$/ICAM-1$^{+/+}$ or ApoE$^{-/-}$/ICAM-1$^{-/-}$ mice fed an atherogenic diet for 4 weeks and the aorta was harvested. **A)** ICAM-1 mRNA was quantified by RT-PCR in mRNA isolated from whole aorta. Values are expressed as means ± SEM. **=p<0.01 versus ApoE$^{-/-}$/ICAM-1$^{+/+}$ + vehicle; ***=p<0.001 versus ApoE$^{-/-}$/ICAM-1$^{+/+}$ + ALDO. **B)** Representative immunostaining (red staining, arrows) for ICAM-1 in aortic root sections in vehicle- or ALDO-treated ApoE$^{-/-}$ mice fed an atherogenic diet for 4 weeks. N=6 for each treatment and genotype for the whole figure.

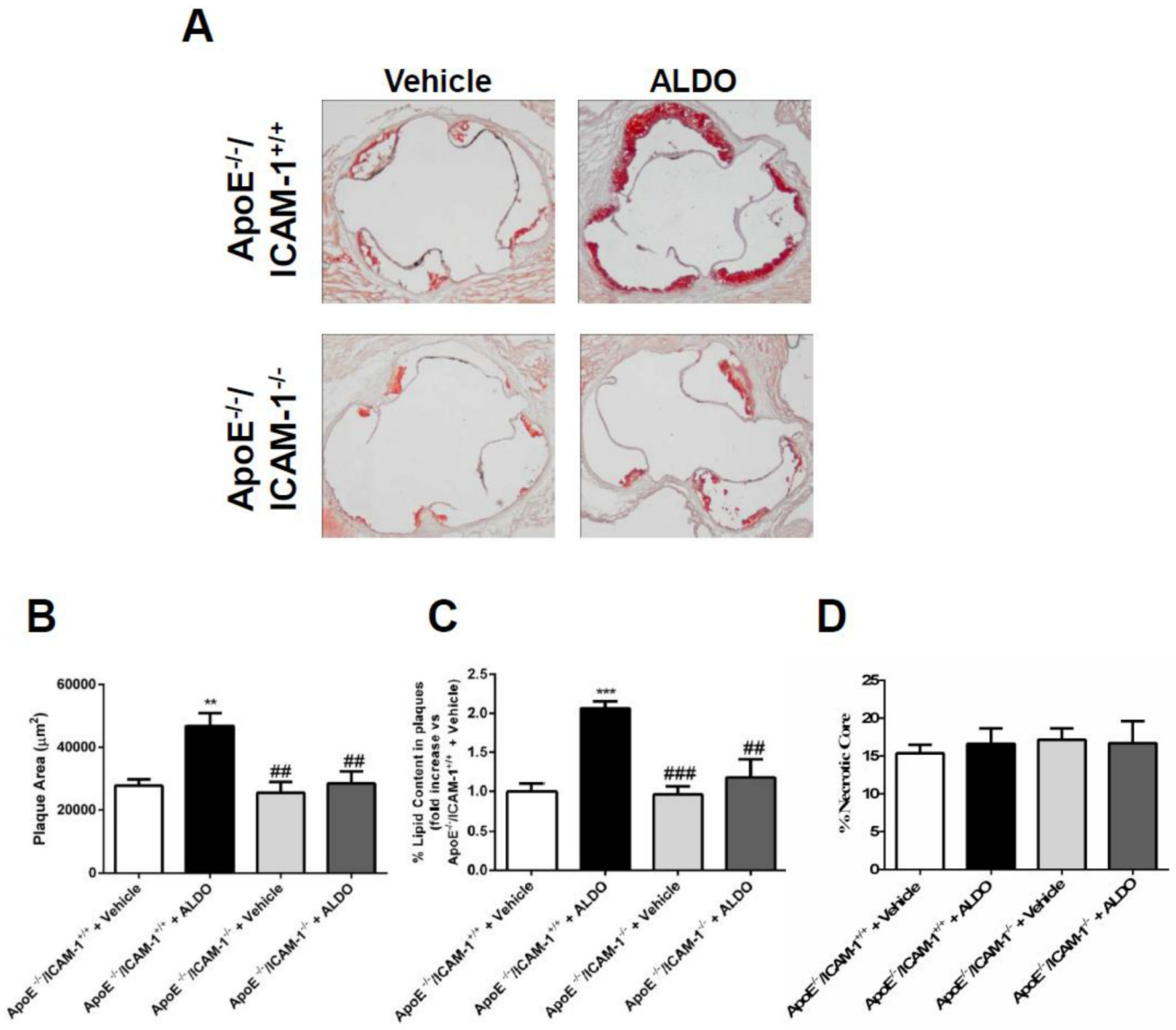

Fig. 2. ICAM-1 is required for early ALDO-induced atherosclerosis development

A, Aortic roots from Aldosterone (ALDO)- or vehicle-infused ApoE$^{-/-}$/ICAM-1$^{+/+}$ or ApoE$^{-/-}$/ICAM-1$^{-/-}$ mice fed an atherogenic diet for 4 weeks were harvested. Sections were stained with Oil-red-O and plaque area, (**B**) percentage of the plaque area that stains positive for lipids (**C**) and percentage of the plaque composed of necrotic core (**D**) were compared between genotypes and treatments. Values are expressed as means ± SEM. **=p<0.01, ***=p<0.001vs vs ApoE$^{-/-}$/ICAM-1$^{+/+}$ + vehicle; ##=p<0.01, ###=p<0.001 vs ApoE$^{-/-}$/ICAM-1$^{+/+}$ + ALDO. N=12 per genotype and treatment.

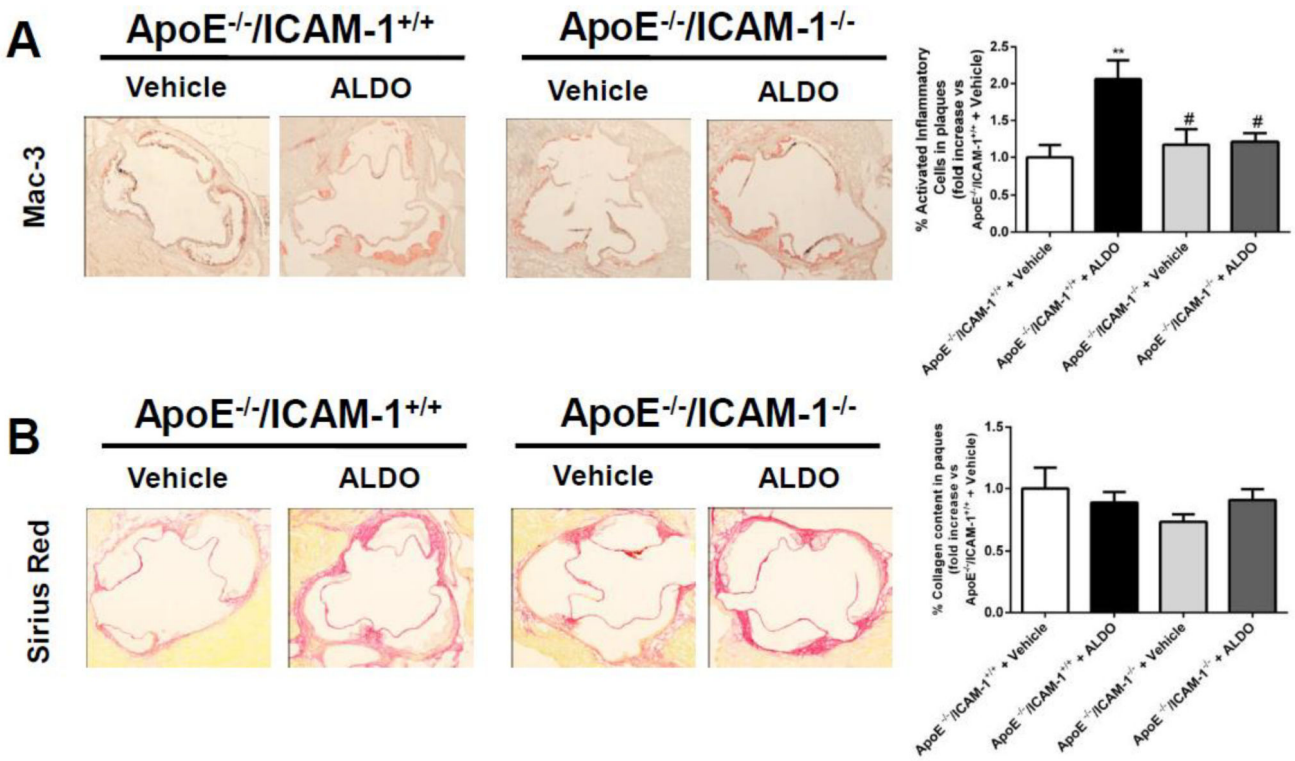

Fig. 3. ICAM-1 is necessary for aldosterone to produce plaques with increased inflammation

Aldosterone (ALDO) or vehicle was infused into ApoE$^{-/-}$/ICAM-1$^{+/+}$ or ApoE$^{-/-}$/ICAM-1$^{-/-}$ mice fed an atherogenic diet for 4 weeks and the aortic root was harvested, and sectioning was performed. Mac3 immunostaining was used to label inflammatory cells and picrosirius red staining was used to quantify fibrosis. The percentage of the plaque area that stained positive for activated inflammatory cells (anti-Mac3 antibody, **A**) and collagen (Sirius Red, **B**) was compared between genotypes and treatments. Data was expressed as fold increase compared with ApoE$^{-/-}$/ICAM-1$^{+/+}$ + vehicle. Values are represented as means ± SEM. **=p<0.01 vs ApoE$^{-/-}$/ICAM-1$^{+/+}$ + vehicle; #=p<0.05 vs ApoE$^{-/-}$/ICAM-1$^{+/+}$ + ALDO. N=12 mice per genotype and treatment.

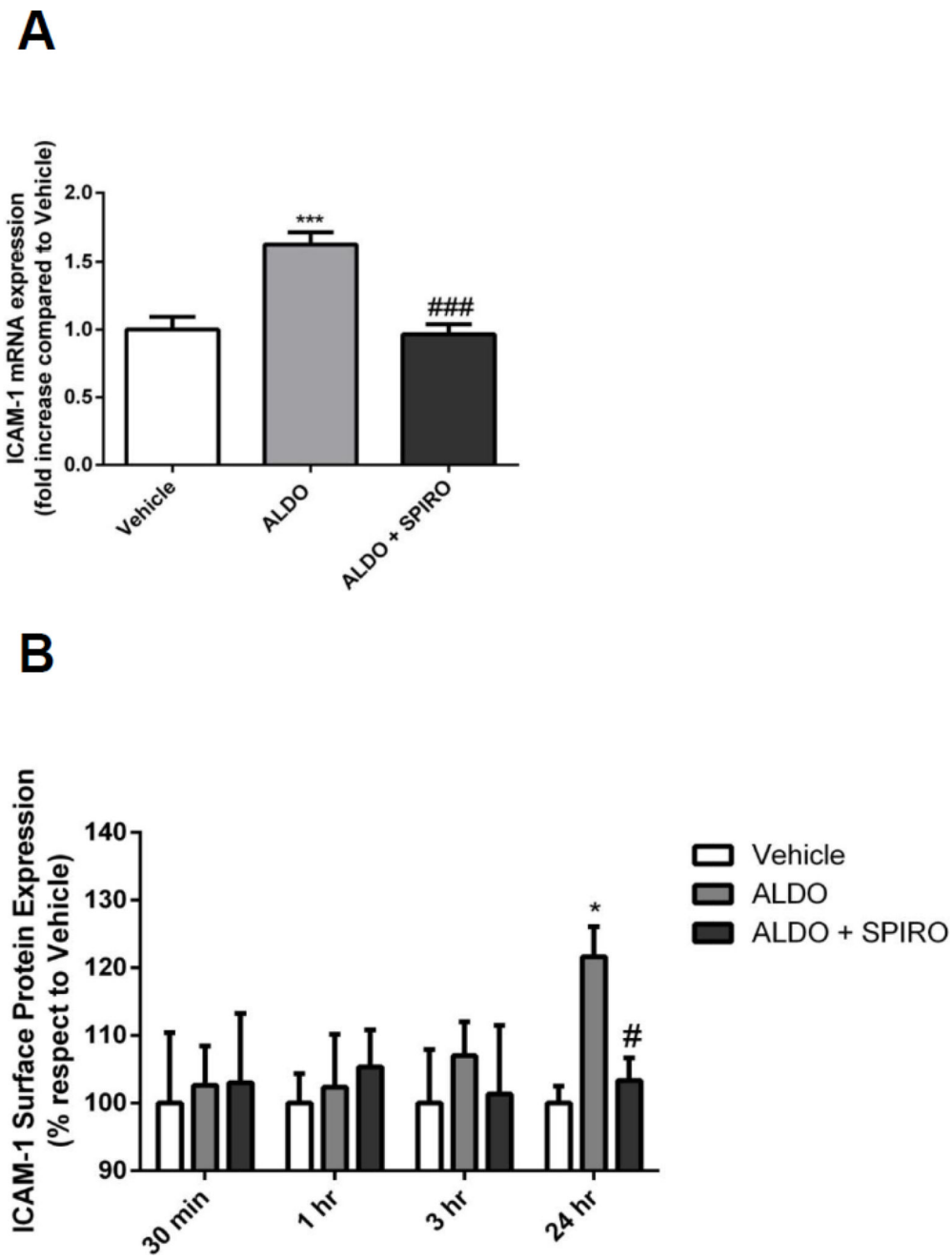

Fig. 4. MR regulates ICAM-1 mRNA and protein expression in human endothelial cells in a genomic time frame

A, Human umbilical vein endothelial cells (HUVEC) were treated with vehicle or aldosterone (ALDO ;10^{-8}M) or ALDO + spironolactone (SPIRO ; 10^{-5}M) for 24 hours and mRNA was quantified by qRT-PCR and expressed as fold-increase versus vehicle. ***=p<0.001 versus Vehicle; ###=p<0.001 versus ALDO. **B,** ICAM-1 surface protein was measured by flow cytometry and expressed as percentage of vehicle-treated cells at each time point. Values are represented as means ± SEM in the whole figure. *=p<0.05 vs 24 hours of vehicle; #=p<0.05 vs 24 hours of ALDO.

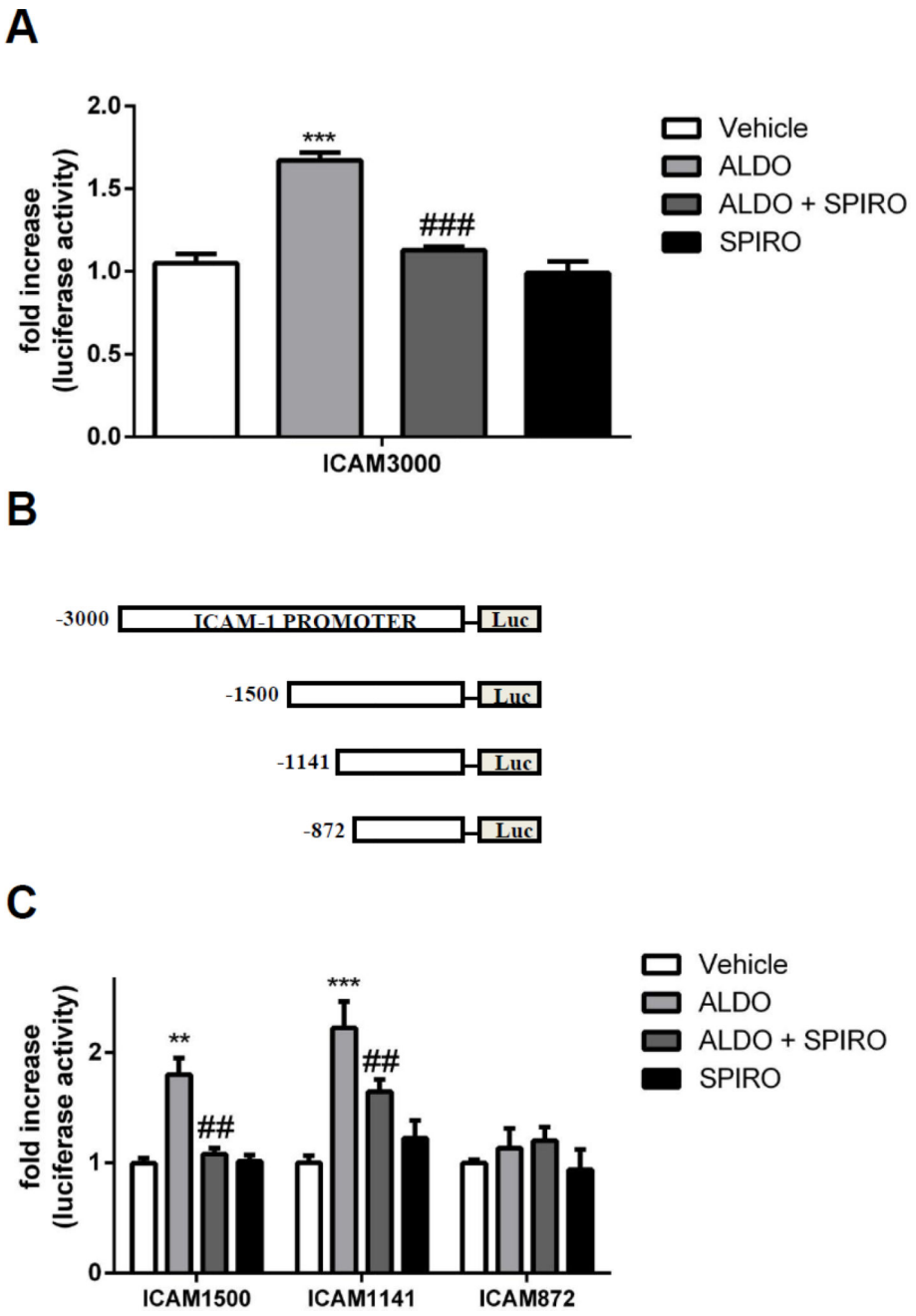

Fig. 5. MR regulates transcription of the human ICAM-1 promoter

A) Human umbilical vein endothelial cells (HUVEC) were transfected with a luciferase reporter containing the 3Kb promoter of human ICAM-1 gene. Transfected HUVECs were treated with vehicle, aldosterone (ALDO 10^{-8}M), ALDO + spironolactone (SPIRO; 10^{-5}M) or SPIRO alone. Luciferase activity was expressed as fold increase compared to Vehicle. ***=p<0.001 versus vehicle and ###=p<0.001 versus ALDO. **B)** Schematic representation of ICAM-1 promoter fragments. **C)** Transcriptional activity of a series of 5' ICAM-1 deleted promoter fragments. HUVECs, transfected with different promoter fragments, were treated with vehicle, ALDO (10^{-8}M), ALDO + SPIRO (10^{-5}M) and SPIRO. The luciferase activity

was expressed as fold increase compared to Vehicle. **=p<0.01, ***=p<0.001 versus vehicle and #=p<0.05, ##=p<0.01 versus ALDO. Values are expressed as means ± SEM in the whole figure. N = 3 independent experiments.

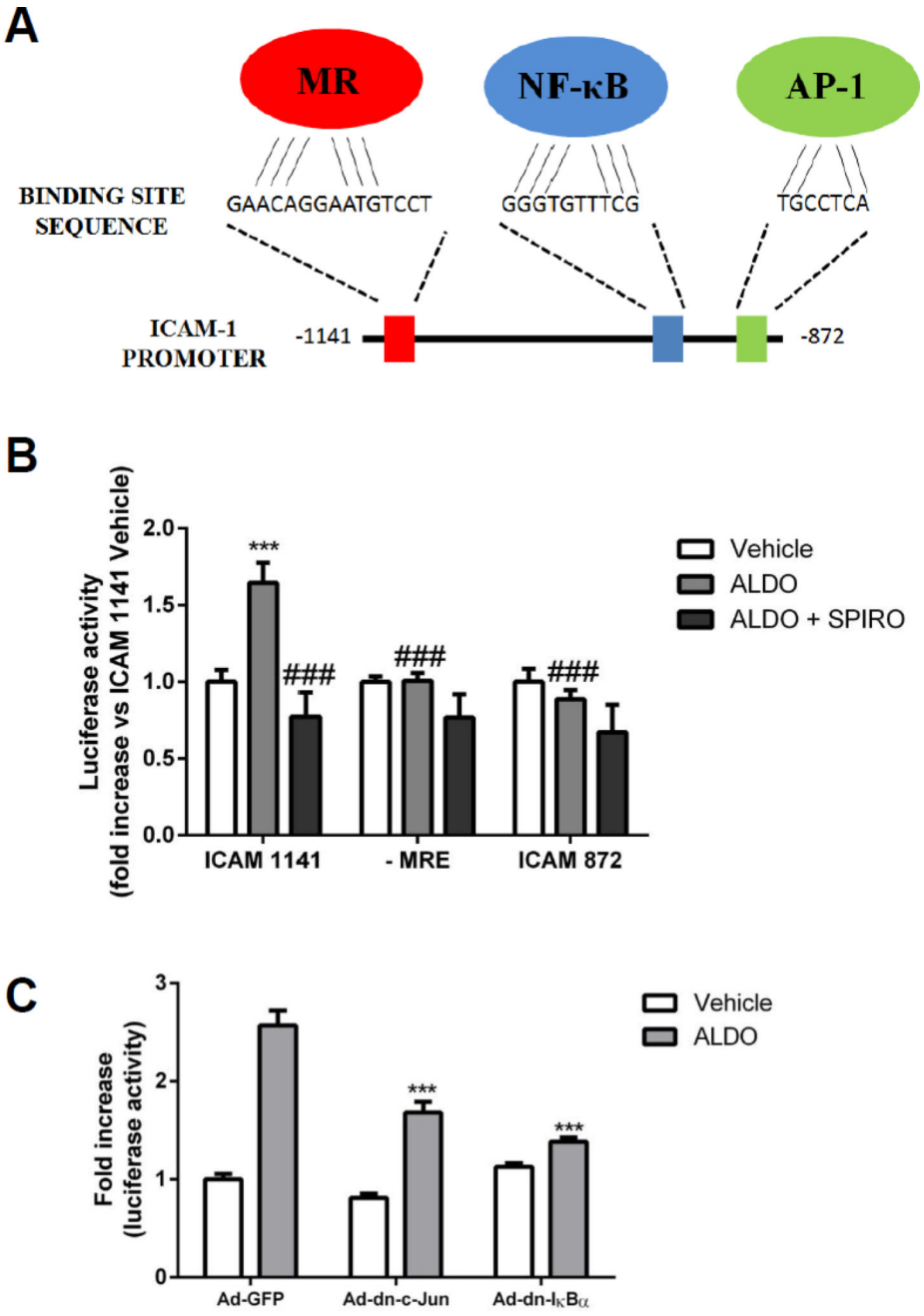

Fig. 6. A predicted mineralocorticoid receptor responsive element in the ICAM-1 promoter is necessary for MR-induced transcriptional activity

A) Schematic representation of putative binding sites for known transcription factors determined by bioinformatic analysis of ICAM-1 promoter region between 1141 bp and 872 bp. **B)** Human umbilical vein endothelial cells (HUVEC) were transfected with luciferase reporter constructs containing the intact 1141Kb promoter of human ICAM-1 gene and with the predicted MR responsive element (MRE) deleted. Transfected HUVECs were treated with vehicle, aldosterone (ALDO 10^{-8}M) or ALDO + spironolactone (SPIRO; 10^{-5}M). Luciferase activity was expressed as fold increase compared to Vehicle. ***=p<0.001 versus

Vehicle and ###=p<0.001 vs ICAM1141 + ALDO. **C)** Promoter activity of the 1141bp ICAM-1 promoter fragment after infection with dominant negative (dn) constructs. After infection with Ad-GFP, Ad-dn-c-Jun and Ad-dn-IκBα, HUVECs were transfected with ICAM1141 promoter fragment and treated with vehicle or ALDO (10^{-8}M). The luciferase activity was expressed as fold increase compared to Vehicle Ad-GFP. ***=p<0.001 versus Vehicle Ad-GFP. N = 3 independent experiments.

Table 1

Cardiovascular risk parameter evaluation in ApoE$^{-/-}$/ICAM-1$^{+/+}$ and ApoE$^{-/-}$/ICAM-1$^{-/-}$mice treated with vehicle or ALDO.

Genotype	ApoE−/−/ICAM-1+/+		ApoE−/−/ICAM-1−/−	
Treatment	**Vehicle (n)**	**ALDO (n)**	**Vehicle (n)**	**ALDO (n)**
Prerandomization				
Weight, g	26.3±0.6 (18)	24.7±0.5 (20)	24.8±0.5 (16)	25.5±0.7 (17)
After 4 weeks of infusion				
Weight, g	28.6±0.7 (18)	27.6±0.5 (19)	28.9±0.6 (16)	27.5±0.7 (17)
Blood glucose, mg/dL	173±8 (8)	185±7 (8)	170±10 (8)	179±9 (8)
Serum Cholesterol, mg/dL	572±18	535±20	564±25	538±28
Serum ALDO, nmol/L	1.28±0.3	4.07±0.7**	1.32±0.4	4.19±0.3**
Serum Sodium, mEq/L	143.8±0.8	148.2±1*	144.5±1.2	149.0±0.9*
Serum Potassium, mEq/L	3.98±0.2	3.01±0.1*	4.01±0.5	3.09±0.4*
Systolic BP, mm Hg	104±3.5 (6)	111.0±2.7 (6)	106±6.8 (6)	112.9±5.1 (6)
Diastolic BP, mmHg	73±1.7 (6)	79.7±1.3 (6)	73.9±6.2 (6)	79.9±5.2 (6)
Heart Rate, pulse/min	532.9±26.2 (6)	582.4±47.6 (6)	513.7±52 (5)	579.8±35.6 (6)

*=p<0.05,

**=p<0.01 ALDO versus Vehicle in the same genotype.